The unstable CO_2 feedback cycle on ocean planets

D. Kitzmann,[1][*] Y. Alibert,[1][*][†] M. Godolt,[2] J. L. Grenfell,[2] K. Heng,[1] A. B. C. Patzer,[3] H. Rauer,[2,3] B. Stracke[2] and P. von Paris[4,5]

[1]*Physikalisches Institut and Center for Space and Habitability, Universität Bern, CH-3012 Bern, Switzerland*
[2]*Institut für Planetenforschung, Deutsches Zentrum für Luft- und Raumfahrt (DLR), D-12489 Berlin, Germany*
[3]*Zentrum für Astronomie und Astrophysik, Technische Universität Berlin, D-10623 Berlin, Germany*
[4]*Univ. Bordeaux, LAB, UMR 5804, F-33270 Floirac, France*
[5]*CNRS, LAB, UMR 5804, F-33270 Floirac, France*

ABSTRACT

Ocean planets are volatile-rich planets, not present in our Solar system, which are thought to be dominated by deep, global oceans. This results in the formation of high-pressure water ice, separating the planetary crust from the liquid ocean and, thus, also from the atmosphere. Therefore, instead of a carbonate–silicate cycle like on the Earth, the atmospheric carbon dioxide concentration is governed by the capability of the ocean to dissolve carbon dioxide (CO_2). In our study, we focus on the CO_2 cycle between the atmosphere and the ocean which determines the atmospheric CO_2 content. The atmospheric amount of CO_2 is a fundamental quantity for assessing the potential habitability of the planet's surface because of its strong greenhouse effect, which determines the planetary surface temperature to a large degree. In contrast to the stabilizing carbonate–silicate cycle regulating the long-term CO_2 inventory of the Earth atmosphere, we find that the CO_2 cycle feedback on ocean planets is negative and has strong destabilizing effects on the planetary climate. By using a chemistry model for oceanic CO_2 dissolution and an atmospheric model for exoplanets, we show that the CO_2 feedback cycle can severely limit the extension of the habitable zone for ocean planets.

Key words: astrobiology – planets and satellites: atmospheres – planets and satellites: oceans – planets and satellites: terrestrial planets.

1 INTRODUCTION

The question of habitability for exoplanets is usually linked to the concept of the so-called habitable zone (HZ), i.e. the range of orbital distances around a host star, where a rocky/terrestrial planet can in principle maintain liquid water on its surface over an extended period of time. Liquid water is – to our current knowledge – one of the most important requirement for life as we know it (e.g. Lammer et al. 2009). However, the classical HZ as introduced by Kasting, Whitmire & Reynolds (1993) is strictly defined for an Earth-like planet, i.e. for a planet with a partially rocky surface, a water content of one Earth ocean, plate tectonics, and with all the geological cycles (in particular, the carbonate–silicate cycle) as on Earth. Given the diversity of the already known exoplanets, it is highly unlikely that the majority of the low-mass planets are entirely Earth-like and can be described within the concept of the classical HZ.

One particular, highly interesting class of exoplanets are ocean planets (or waterworlds), i.e. planets with a much higher water content than Earth. Several candidates for massive water-rich planets have already been found. Due to their small orbital distances, none of these can be considered to be a potential habitable planet, though. The most well-studied example so far is the transiting super-Earth GJ1214 b (Charbonneau et al. 2009). Its mean density derived from observations suggests that roughly half the planet's bulk composition could be made of water. In general, the larger radii of ocean planets compared to more rocky planets of equal mass (Léger et al. 2004; Alibert 2014) would make them very interesting targets for planet detection and characterization with, for example, *CHEOPS* (*CHaracterising ExOPlanet Satellite*; Fortier et al. 2014), *TESS* (*Transiting Exoplanet Survey Satellite*; Ricker et al. 2014), *PLATO* (*Planetary Transits and Oscillations of stars*; Rauer et al. 2014) or the *JWST* (*James Webb Space Telescope*; Gardner et al. 2006). Being completely covered by a deep water envelope, they fall within the apparent gap between terrestrial planets with a (partially) rocky surface and the gas giant planets with a high amount of hydrogen and helium.

In this study we focus on the potential habitability of low-mass deep ocean planets. First considered by Léger et al. (2004), these

[*]E-mail: daniel.kitzmann@csh.unibe.ch (DK); yann.alibert@space.unibe.ch (YA)
[†]On leave from CNRS, Observatoire de Besançon, 41 avenue de l'Observatoire, 25000 Besançon, France.

types of planets would form beyond the ice line within a protoplanetary disc, where they collect a large fraction of water as well as other volatiles as ices and later migrate inwards into the HZ (Kuchner 2003). These considerations are supported by the results from planetary formation models, where migrated terrestrial low-mass planets with a large water inventory ($>$100 Earth oceans) located in the classically defined HZ are a very common result (Alibert et al. 2013; Alibert 2014; Thiabaud et al. 2014).

Studies on the internal structure of such planets by Léger et al. (2004) and Alibert (2014) suggest that they will have ocean depths in excess of 100 km, which makes the presence of a continental landmass highly unlikely. Categorized as Class IV habitats by Lammer et al. (2009) these planets can offer one of the most important requirements for life: liquid water. Of course, such a large reservoir of water (H$_2$O) also influences climate processes. One important consequence is, for example, the formation of high-pressure water ice (ice phases VI and VII) at the bottom of the ocean, which prevents the immediate contact of the planetary crust with the liquid ocean. Thus, the well-known carbonate–silicate cycle (Walker, Hays & Kasting 1981; Kasting, Whitmire & Reynolds 1993) is unable to operate as a long-term climate stabilization mechanism regulating the atmospheric carbon dioxide content. Abbot, Cowan & Ciesla (2012) also showed that below a landmass fraction of 1 per cent, the usual seafloor weathering, which is an important part of the carbonate–silicate cycle, becomes inoperative, such that the stabilizing weathering-climate feedback on ocean planets does not work even if the liquid ocean is still in contact with the planetary crust.

Since the ocean planet originates from beyond the ice line in the protoplanetary disc, the total amount of CO$_2$ accumulated during its formation is also thought to be much higher than the Earth's inventory (see e.g. Léger et al. 2004; Alibert 2014; or Marboeuf et al. 2014). As discussed in Léger et al. (2004), the CO$_2$ amount present above the high-pressure water ice layer may, however, be strongly limited by gravitational sequestration during the planetary formation (i.e. most of the CO$_2$ is trapped below the water ice layer), clathrate formation or atmospheric loss. In case of negligible atmospheric loss processes of CO$_2$ or very inefficient formation of CO$_2$−H$_2$O clathrates, the total (initial) inventory of CO$_2$ present in the ocean and the atmosphere remains constant over time, because CO$_2$ cannot interact with the planetary interior via subduction or outgassing. Then, the partial pressure of CO$_2$ in the atmosphere is purely determined by its partial dissolution in the liquid ocean.

Note that the occurrence of convection and plate tectonics within the ice mantle is quite uncertain. Studies by Fu, O'Connell & Sasselov (2010) or Levi, Sasselov & Podolak (2014) suggest the possibility of ice mantle convection on ocean planets under certain conditions. Convection depends on details such as the temperature profile within the ice mantle, the planet's interior heat loss over time or the viscosity of the high-pressure ice phases. Given the uncertainties in, for example, the experimental data of the ice viscosity or the detailed evolution of the planetary interior, it is currently not possible to constrain the occurrence of a convective ice mantle over the lifetime of the planet. Additionally, it was shown by Levi et al. (2014) that methane (CH$_4$) could be transported through the convective ice mantle in the form of clathrates. To our knowledge, no theoretical or experimental data are available on clathrate formation for CO$_2$ under the conditions encountered on an ocean planet. Assuming an efficient transport of carbon dioxide clathrates through the convective ice mantle would, in principle, connect the oceanic and atmospheric CO$_2$ with the CO$_2$ reservoir below the ice mantle. It is a priori not clear, if such a connection would work as a long-term stabilization (as on Earth) or would even further enhance the CO$_2$ effect discussed in this study. Due to these uncertainties, we assume that no transport of CO$_2$ through the ice mantle occurs on the ocean planets in our study.

In this study we investigate the interaction of the ocean with the atmospheric CO$_2$. We present a potentially unstable CO$_2$ cycle which, unlike the carbonate–silicate cycle on Earth, acts as a destabilizing climate feedback and might limit the overall habitability of an ocean planet. Oceanic dissolution of CO$_2$ is also a well-known effect in Earth climatology. The oceanic water of Earth has an overall CO$_2$ content of about 2 bar (Pierrehumbert 2010), which is much more than its actual corresponding atmospheric partial pressure of roughly 10^{-4} bar. The increased anthropogenic release of CO$_2$ into the atmosphere results in an ocean acidification which will considerably lower the pH value of the Earth ocean within the next centuries (Caldeira & Wickett 2003). While this will have a strong effect on the maritime biosphere in near future, the overall impact on the atmosphere and surface temperature is limited to a few kelvin because of the small size of the Earth oceans (compared to ocean planets) and the long-term stabilization via the carbonate–silicate cycle.

While ocean planets can in principle be more massive, we limit our present study to planets with the mass and radius of the Earth, orbiting a Sun-like star, as first example. Otherwise, we would need additional assumptions on the bulk composition and internal structure of the ocean planet to derive a corresponding mass–radius relationship. This, however, is not the topic of this study which focuses on the impact of the temperature-dependent dissolution of CO$_2$ in the ocean on the planetary habitability. The results of this study are also directly applicable to ocean planets with higher masses and radii, though. We assume that any initially accumulated hydrogen and helium is already lost, which is a reasonable assumption for low-mass planets (Lammer et al. 2008; Alibert 2014).

The details of the model for the oceanic CO$_2$ dissolution are described in Section 2. In Section 3, we discuss the atmospheric model and employ it to study the habitability of ocean planets.

2 OCEANIC CO$_2$ DISSOLUTION

Both the amount of liquid ocean water (i.e. the size of the global ocean) as well as the dissolved CO$_2$ within the ocean (and thus also the atmospheric CO$_2$ content) are in general a function of temperature. Thus, we derive the size of the liquid ocean and describe the chemistry for the dissolution of CO$_2$ in ocean water in this section. We thereby do not account for loss processes of atmospheric CO$_2$ to space or for the potential formation of CO$_2$−H$_2$O clathrates as both of them are hard to quantify without more additional assumptions.

2.1 Ocean mass

In the following, we assume that the ocean is isothermal with a temperature equal to the temperature at the ocean's surface to study the lower limit of the CO$_2$ feedback impact on the atmospheres of low-mass ocean planets. This assumption results in the smallest possible ocean size. If, for example, an adiabatic temperature profile had instead been adopted (Léger et al. 2004), the ocean would have been larger and able to store a larger quantity of CO$_2$. This on the other hand would amplify the proposed CO$_2$ feedback mechanism as discussed below.

Assuming an isothermal ocean, its maximal mass is constrained by the maximum pressure of liquid water, given by the temperature- and pressure-dependent melting curves of water ice phases VI

Table 1. Simon–Glatzel equation parameters for the melting curves of water ices.

Ice phase	Triple point parameters		Power-law parameters	
	p_0 (MPa)	T_0 (K)	a (MPa)	c
Ice VI[a]	618.4	272.73	661.4	4.69
Ice VII[b]	2216	355	534	5.22

Notes. [a]Choukroun & Grasset (2007), [b]Alibert (2014).
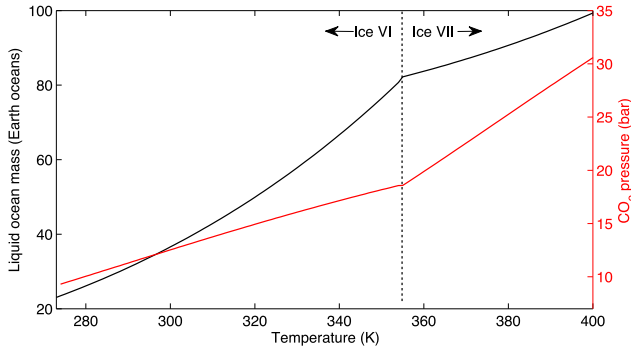
Figure 1. Mass of the liquid ocean and total atmospheric CO_2 pressure as a function of isothermal ocean temperature. The atmospheric CO_2 partial pressure (red line) is shown for a total CO_2 inventory of 10^{21} kg and 10^{18} kg of N_2. The vertical dotted line indicates the boundary between the formation of the ice phases VI and VII at the ocean's bottom.

and VII. This maximum pressure p is described as a function of temperature T by the empirically derived Simon–Glatzel equation (Simon & Glatzel 1929)

$$p = p_0 + a \left(\left(\frac{T}{T_0} \right)^c - 1 \right), \tag{1}$$

where p_0 and T_0 are reference values (usually the corresponding triple points) and a and c are power-law parameters obtained from experimental data. The corresponding parameters for the equation are summarized in Table 1 and have been adopted from Alibert (2014) for ice phase VII and from Choukroun & Grasset (2007) for ice VI.
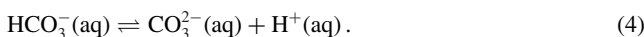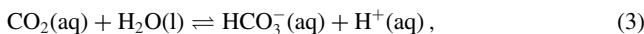
The ocean mass is shown in Fig. 1 as a function of (isothermal) temperature. It varies considerably from about 25 to 100 Earth oceans between 273 and 400 K. Thus, at low temperatures, less liquid water is available to dissolve the atmospheric CO_2.

2.2 CO_2 dissolution model

Following the description of Pierrehumbert (2010), we derive the atmospheric CO_2 content by taking into account the dissolution of CO_2 within the ocean. In equilibrium, the atmospheric partial pressure of $CO_2(g)$, $p_{CO_2(g)}$, and the concentration of $CO_2(aq)$ dissolved in the ocean ($c_{CO_2(aq)}$) are linked by Henry's law

$$p_{CO_2(g)} = K_H(T) \cdot c_{CO_2(aq)} \tag{2}$$

with the temperature-dependent Henry's law constant $K_H(T)$. Additional reactions occurring within the ocean convert the dissolved $CO_2(aq)$ into hydrogen carbonate (HCO_3^-) and carbonate (CO_3^{2-})

$$CO_2(aq) + H_2O(l) \rightleftharpoons HCO_3^-(aq) + H^+(aq), \tag{3}$$

$$HCO_3^-(aq) \rightleftharpoons CO_3^{2-}(aq) + H^+(aq). \tag{4}$$

The hydrogen ion H^+ is additionally linked to the hydroxide ion OH^- via the dissociation reaction of water

$$H_2O(l) \rightleftharpoons H^+(aq) + OH^-(aq). \tag{5}$$

Assuming chemical equilibrium, we solve this system under the constraint of charge balance

$$\left[H^+ \right] = \left[HCO_3^- \right] + 2 \left[CO_3^{2-} \right] + \left[OH^- \right] \tag{6}$$

by using a Newton–Raphson method, iterating the mole concentration [H+]. Rate constants for the chemical reactions and Henry's law have been taken from Pierrehumbert (2010). The temperature dependence of the reaction rates are described via the Arrhenius equation. The rate coefficients used here are defined for an Earth-like oceanic salinity of 30 per cent. The salinity can have a large effect on the rates of the reactions (3) and (4). Tests with low-salinity rate constants (taken from the supplementary material of Pierrehumbert 2010) indicate that our results are mostly insensitive to the oceanic salinity. In the cases studied in this paper, most of the carbon is stored as dissolved CO_2 in the ocean, such that the reactions (3) and (4) are only of minor importance.

Note that [H+], when expressed in units of moles per litre, is associated with the pH value of the ocean via

$$pH_{ocean} = -\log_{10} \left[H^+ \right]. \tag{7}$$

Given a total CO_2 mass inventory $m_{CO_2,tot}$, a second Newton–Raphson method is applied to find the atmospheric mass of CO_2 ($m_{CO_2(g)}$) for which the conservation of mass

$$m_{CO_2,tot} = m_{CO_2(g)} + m_{CO_2(aq)} \tag{8}$$

is achieved, where $m_{CO_2(aq)}$ is determined by the chemical system described above as a function of $p_{CO_2(g)}$. Atmospheric mass and partial pressure of $CO_2(g)$ are related via the condition of hydrostatic equilibrium.

We do not consider the presence of positive calcium ions (Ca^{2+}) in the charge balance. On planets such as Earth, these ions can originate from the dissolution of limestone ($CaCO_3$) in water

$$CaCO_3(s) \rightleftharpoons Ca^{2+}(aq) + CO_3^{2-}(aq). \tag{9}$$
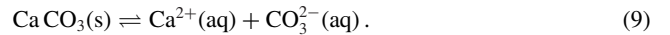
Since, however, the liquid water on the planets under consideration is not in contact with a rocky surface, this source for the Ca^{2+} ions does not exist. Note that adding Ca^{2+} ions via dissolved limestone would strongly increase the capability of the ocean to take up CO_2 and, thereby, enhance the CO_2 feedback cycle.[1]

2.3 Results

Fig. 1 shows the resulting atmospheric partial pressure $CO_2(g)$ as a function of isothermal ocean temperature for a total inventory of 10^{21} kg as a particular example for an intermediate value of the range of CO_2 inventories considered in the following. The atmospheric mass of nitrogen (N_2) is fixed at an approximately Earth-like value of 10^{18} kg. For this example, the surface pressure of $CO_2(g)$ increases from about 9 bar at 273 K to more than 30 bar at 400 K. Taking into account the results of planetary population synthesis models from e.g. Marboeuf et al. (2014) to constrain the overall amount of CO_2 accumulated from the protoplanetary disc for low-mass planets which have migrated into the HZ, we vary the total CO_2 inventory between 10^{16} and 10^{24} kg. The results are presented in

[1] This is of course also true for all other influences affecting the charge balance in equation (6).
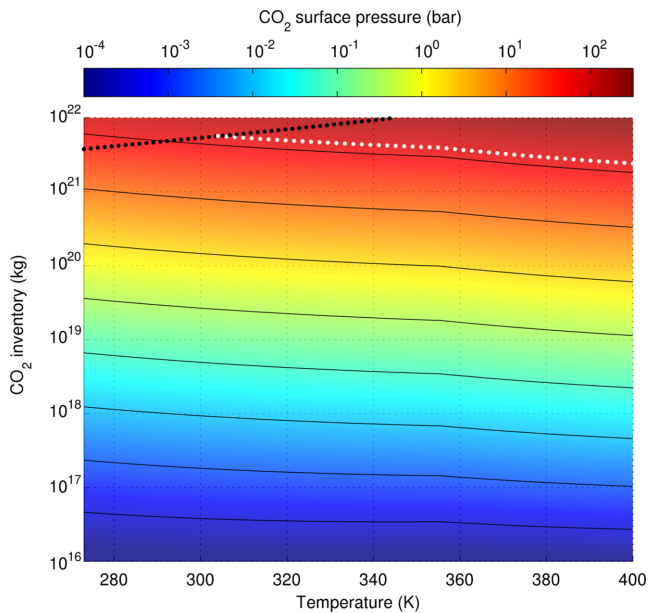
Figure 2. Atmospheric partial pressure of CO$_2$ as a function of ocean temperature and total CO$_2$ inventory. The amount of N$_2$ in the atmosphere is fixed at 10^{18} kg in each case. The solid, black lines represent contour lines for constant CO$_2$ pressures. The condensation limit for CO$_2$ is indicated by the dotted line. Atmospheric partial pressures of CO$_2$ above that line are thermodynamically unstable and would condense out. The white, dotted line marks the critical point limit of CO$_2$. Above this limit, the treatment of the equilibrium chemistry becomes unsuitable.

Fig. 2, where a N$_2$ inventory of 10^{18} kg is used again in each case.

We note that the results in Fig. 2 for very high total CO$_2$ inventories are physically unrealistic as they predict atmospheric partial pressures of more than 100 bar. Such a large amount of CO$_2$(g) would partially condense on to the surface as liquid CO$_2$. According to the vapour pressure curve (Ambrose 1956), the highest partial pressure of CO$_2$(g) at 400 K is roughly 600 bar while at 273 K only about 34.7 bar can be stable in the atmosphere in gaseous form. The condensation limit is indicated by the dotted, black line in Fig. 2. Atmospheric partial pressures of CO$_2$ above that line are thermodynamically unstable and would condense out, removing it from the atmosphere (see also von Paris et al. 2013c). Additionally, some of the results shown in Fig. 2 lie above the critical point of CO$_2$, which is located at a temperature of 304.25 K and pressure of 73.8 bar. Above the critical point, the description of the equilibrium chemistry from Section 2.2 is probably unsuitable and the corresponding results should be treated with great care. The critical point limit is indicated by the dotted, white line in Fig. 2. We note that none of these unrealistic values are used for the atmospheric model calculations in Section 3.

In general, the CO$_2$(g) partial pressure varies over several orders of magnitudes across the parameter space. Even though, the ocean is smaller at low temperatures and, thus, less liquid water is available to dissolve the atmospheric CO$_2$, the temperature dependence of the dissolution is stronger. The ability of the ocean to dissolve CO$_2$ decreases with increasing temperature, which leads to a positive, and thus potentially destabilizing, feedback cycle within the atmosphere. The partial pressure of CO$_2$(g) likewise decreases with temperature owing to the ability of the ocean to dissolve a larger amount of CO$_2$ at lower temperatures. This, again results in a positive feedback cycle.

Thus, at low surface temperatures, where CO$_2$ would be required as an atmospheric greenhouse gas to heat the planetary surface, the ocean binds an increasing amount of CO$_2$ and, thereby, removes the important greenhouse gas from the atmosphere. For higher temperatures on the other hand, less CO$_2$ can be dissolved in the ocean and starts to accumulate in the atmosphere, contributing to the greenhouse effect and further increasing the surface temperature. In contrast to the stabilizing carbonate–silicate cycle operating on Earth, this therefore induces positive feedback cycles, which could lead to potentially unstable situations: an atmospheric freeze-out with a runaway glaciation or a runaway greenhouse effect, for example. This is directly comparable to the water vapour feedback where the atmospheric content of H$_2$O increases strongly with surface temperature, which may finally result in a runaway greenhouse process (Komabayashi 1967; Kasting 1988). These positive CO$_2$ feedback cycles will obviously have important implications for the potential habitability of an ocean planet. This effect has also been noted in the appendix of Wordsworth & Pierrehumbert (2013) as a possibly important mechanism on volatile-rich planets.

The highest surface temperatures considered in this study are limited to 400 K, assuming that this is the limit for microorganisms to survive and thus a potential limit for the presence of life as we know it (Cockell 1999; Rothschild & Mancinelli 2001; Lammer et al. 2009). The lowest surface temperature for the limit of potential habitability is considered to be the freezing point of water (273 K). Note that 3D studies show that the global mean surface temperature of 273 K may still allow for liquid water in the equatorial region (see e.g. Wolf & Toon 2013; Kunze et al. 2014)

3 ATMOSPHERIC MODEL CALCULATIONS

Since the planetary surface temperature depends – amongst other things – on the atmospheric amount of CO$_2$ which, as described above, is a function of the oceans temperature, we use an atmospheric model coupled with the CO$_2$(aq) dissolution model to constrain the potential habitability of the ocean planet. The one-dimensional, radiative–convective atmospheric model was developed for terrestrial planets and is described in the next subsection. The results from the model calculations using the dissolution model and the atmospheric model are shown in Section 3.2. Focusing on the CO$_2$ feedback mechanism, we present the model calculations for a G2V host star: the Sun. However, this study can of course be applied to other central stars straightforwardly. The atmospheric composition for this study is restricted to a mixture of water, carbon dioxide, and molecular nitrogen. The atmospheric amount of N$_2$ remains fixed at an approximately Earth-like value of 10^{18} kg. Nitrogen, unless present in very high amounts, has a very limited effect on the resulting surface temperature (von Paris et al. 2013b; Wordsworth & Pierrehumbert 2013).

3.1 Atmospheric model description

For the atmospheric model calculations we use a modified version of the one-dimensional radiative–convective atmospheric model extensively described in Kitzmann et al. (2010) and von Paris et al. (2010). The model has been updated in Stracke et al. (2015) to include new absorption coefficients in the shortwave part of the radiative transfer based on the HITEMP2010 data base (Rothman et al. 2010). The model considers CO$_2$, H$_2$O and N$_2$ as atmospheric gases, neglecting other, potentially important, radiative trace species which might be present, such as O$_2$, SO$_2$, O$_3$ or CH$_4$.

Nitrogen and CO_2 are assumed to be well mixed throughout the atmosphere. Water vapour profiles for low surface temperatures are calculated by the fixed relative humidity profile of Manabe & Wetherald (1967) through the troposphere. For the water-rich atmospheres at high stellar insolations, a relative humidity of unity is used (Kasting et al. 1993; Kopparapu et al. 2013). Above the cold trap, the water profile is set to an isoprofile using the H_2O concentration at the cold trap.

The temperature profile is calculated from the requirement of radiative equilibrium by a time-stepping approach, as well as performing a convective adjustment (Manabe & Strickler 1964), if necessary. The convective lapse rate is assumed to be adiabatic, taking into account the condensation of H_2O and CO_2 (Kasting et al. 1993; von Paris et al. 2010).

As described in von Paris et al. (2010), the cloud-free radiative transfer of the atmospheric model is split into two wavelength regimes: a shortwave part, dealing with the wavelength range of the incident stellar radiation and the longwave part for the treatment of the atmospheric thermal radiation. Both parts use the correlated-k method to describe the gaseous opacity. For the shortwave radiative transfer, 38 spectral intervals between 0.238 and 4.55 µm are used, in the longwave part 25 bands from 1 to 500 µm (von Paris et al. 2010). In this wavelength region, only absorption by CO_2 and H_2O is taken into account. Rayleigh scattering is considered for CO_2, N_2 and H_2O (von Paris et al. 2010). Continuum absorption is taken into account for CO_2 in the longwave (von Paris et al. 2010) and H_2O in both wavelength regions (Clough, Kneizys & Davies 1989). The equation of radiative transfer is solved by two-stream methods (Toon et al. 1989). In the shortwave region, a δ-Eddington two-stream method is employed, while in the longwave part a hemispheric-mean two-stream radiative transfer is used (Kitzmann et al. 2010). The spectrum of the Sun describing the incident stellar radiation has been compiled from data published by Gueymard (2004, see Kitzmann et al. 2010 for details). A planetary surface albedo of 0.06 for liquid water is used throughout this study (Li et al. 2006).

3.2 Results

In principle, it is possible to couple the chemical CO_2 dissolution model from Section 2.2 directly with the atmospheric model to calculate the atmospheric content of CO_2 interactively every time step as a function of surface temperature. However, this approach does not reliably converge in every case since one of the main atmospheric greenhouse gases is changed constantly within a positive feedback cycle. This easily leads to runaway scenarios, where CO_2 either accumulates in the atmosphere or is removed until the atmosphere freezes out. Instead of a direct coupling, we use a slightly different approach in this study.

Since the desired surface temperatures are known a priori (273 and 400 K), the atmospheric content of CO_2 is fixed at the corresponding value from the CO_2 dissolution model shown in Fig. 2. With the fixed CO_2 atmospheric partial pressure, the atmospheric model is used to find the corresponding orbital distance where the atmosphere is in thermal equilibrium for the chosen surface temperatures and CO_2 inventories.

The resulting orbital distances for surface temperatures of 273 and 400 K are shown in Fig. 3. We additionally compute the distances for different stellar ages, taking into account the change of the solar luminosity over time (Gough 1981). The results depicted in Fig. 3 suggest that the range of distances for which the ocean planet remains habitable over an extended period of time (6 Gyr) is quite small. It is strongly restricted to CO_2 inventories between
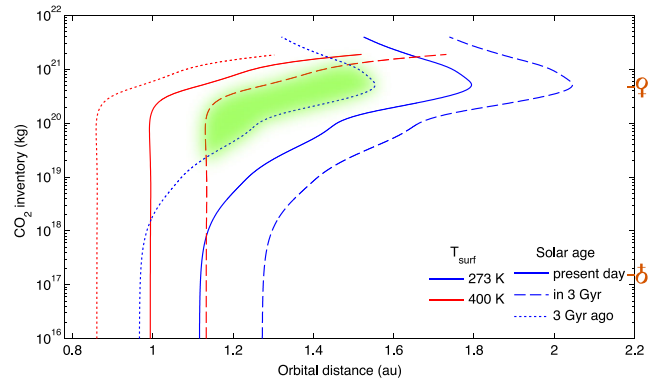

Figure 3. Orbital distances for habitable surface conditions. Coloured lines represent surface temperatures T_{surf} of 273 K (blue) and 400 K (red). Line styles indicate different stellar ages of the Sun. The green area shows the distances and CO_2 inventories for which the planet remains habitable over the entire time period (6 Gyr). The corresponding inventories of $CO_2(g)$ for Venus and $CO_2(g)+CO_2(aq)$ for Earth are indicated at the right-hand axis for comparison.

10^{19} and 10^{21} kg and to orbital distances between 1.1 and 1.5 au. Thus, without the stabilizing carbonate–silicate cycle, the HZ of ocean planets might be much smaller than predicted by the concept of the classical HZ (Kasting et al. 1993; Kopparapu et al. 2013).

At large orbital distances the results are similar to the well-known maximum CO_2 greenhouse effect (Kasting et al. 1993; Kopparapu et al. 2013). In this case, a maximum partial pressure of CO_2 exists where the greenhouse effect still outweighs the Rayleigh scattering, yielding a net heating. For larger partial pressures, however, Rayleigh scattering dominates. Thus, the planet must be located closer to the host star to keep the surface temperature above the freezing point of water. At a temperature of 273 K, the total amount of $CO_2(g)$ which can be present in the atmosphere is restricted to about 34.7 bar (equivalent to roughly 3.7×10^{21} kg of total CO_2), because any additional CO_2 in excess of that partial pressure would condense on to the surface, forming a layer of liquid CO_2 floating on top of the ocean.

For small CO_2 inventories, the planetary conditions at inner distances are mostly determined by the usual water vapour feedback cycle which might eventually lead to a runaway greenhouse effect (however, see Stracke et al. 2015, for new results concerning the runaway greenhouse effect). In contrast to that, the atmospheric partial pressure of CO_2 for larger inventories is sufficient to increase the surface temperature above 400 K already far beyond the current Earth orbit. The positive feedback cycle results here in an atmospheric CO_2 content larger than 30 bar, rendering the planetary surface uninhabitable. These findings imply that ocean planets are most likely continuously habitable only for very specific conditions. The positive feedback cycle of the oceanic CO_2 dissolution severely constrains the potential habitability of these types of planets.

The dissolution of CO_2 in the ocean also has a strong impact on its pH value. Fig. 4 shows the resulting pH values for the two different surface temperatures as a function of total CO_2 inventory. With increasing CO_2 content, more $CO_2(aq)$ is dissolved in the ocean which considerably lowers the pH value by the release of H^+ ions needed to meet the requirement of charge balance (equation 6). Starting at pH values of about 6, it decreases to values of roughly 2.5 for the considered CO_2 inventories. This may, additionally to the temperature effect, have an impact on the potential habitability of the liquid ocean (Rothschild & Mancinelli 2001; Lammer et al.
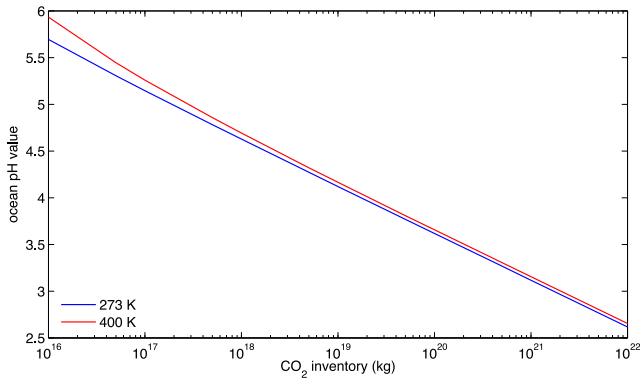
Figure 4. Oceanic pH values as a function of total CO$_2$ inventory. The red line denotes surface temperatures of 400 K, the blue one 273 K.

2009). The pH values for surface temperatures of 400 K are overall lower compared to the one for 273 K. This is related to the fact that at 273 K – even though the liquid ocean is smaller – more CO$_2$ is dissolved in the ocean. Note that even at very low CO$_2$ inventories the ocean of the waterworld has already a much lower pH value than the Earth ocean, with a pH value of about 8. This is caused by the absence of limestone in contact with the ocean planet's liquid water which, when dissolved, would reduce the acidity of the ocean, buffering the pH (Pierrehumbert 2010).

4 SUMMARY

In this study we investigated the potential habitability of extrasolar ocean planets. We focused on the CO$_2$ cycle where the atmospheric CO$_2$ can be partially dissolved in the deep water ocean. The high pressure at the ocean's bottom results in the formation of high-pressure water ices which separate the liquid water from the planetary crust, thus rendering the usual, stabilizing carbonate–silicate cycle inoperable.

We used a chemical equilibrium chemistry to calculate the temperature-dependent dissolution of atmospheric CO$_2$ in the liquid ocean, taking also the change of the ocean's size with temperature into account. The results from the dissolution model imply that the CO$_2$ cycle operating on ocean planets is positive and, thus, potentially destabilizing. The ability of the ocean to dissolve CO$_2$ increases with decreasing temperature. Thus, at low surface temperatures the ocean can bind an increasing amount of CO$_2$ which removes the important greenhouse gas from the atmosphere where it is needed to retain habitable conditions on the surface. For higher temperatures on the other hand, less CO$_2$ can be dissolved in the ocean and starts to accumulate in the atmosphere which results in the build-up of a massive CO$_2$ dominated atmosphere. This greatly contributes to the greenhouse effect, further increasing the surface temperature.

The results of the dissolution model were then used in an atmospheric model for exoplanets to calculate the distances of the ocean planets to their host star where the surface still remains habitable for an extended period of time. We showed that the range of distances is very restricted in terms of the total CO$_2$ inventory of an ocean planet.

These findings imply that ocean planets are most likely continuously habitable only for very specific conditions. The positive feedback cycle of the oceanic CO$_2$ dissolution severely constrains the potential habitability of these types of planets. While this study is focused on carbon dioxide, the same temperature dependent solu-

bility and therefore positive feedback cycles can also be obtained for other important greenhouse gases, such as methane, for example. Thus, our results have important implications for the general question of habitability for exoplanets because the classical concept of the HZ for Earth-like planets which implicitly assumes an operating carbonate–silicate cycle is obviously not applicable to water-rich exoplanets. We note, however, that other – potentially important factors – might influence the results presented in this study. This includes e.g. the potential formation of H$_2$O$-$CO$_2$ clathrates or the transport of CO$_2$ through the ice layer via clathrate diffusion or convection processes within the ice mantle all of which can affect the CO$_2$ content in the ocean and the atmosphere.

Finally, we also want to point out another possible constraint for the habitability of ocean planets. Since these planets migrate from beyond the protoplanetary discs ice line, the water can be initially in a frozen state (Léger et al. 2004) and has to be melted before any secondary atmosphere can be formed. Water ice, however, has a high albedo and, thus, reflects a large fraction of the incident radiation from a solar-type star. In the case that the primordial hydrogen–helium atmosphere (Pierrehumbert & Gaidos 2011), or other processes, such as impacts, the energy acquired during the accretion phase within the disc, or a CO$_2$/CH$_4$ atmosphere outgassed through the ice mantle (Levi et al. 2014), did not result in an initial melting of the water ice, the stellar insolation must then be very high to melt the icy surface and form a liquid ocean. Assuming a conservative ice albedo of 0.5 and present-day solar luminosity, the planet must be located at about 0.74 au to attain a global mean surface temperature of 273 K. At this distance, however, the planet, once the liquid ocean starts to form, would presently undergo a H$_2$O runaway greenhouse scenario (Komabayashi 1967; Kasting 1988), rendering it uninhabitable. Being a potential strong constraint on the habitability of ocean planets, this process warrants further investigation, especially with regard to the ice albedo feedback for different stellar types (von Paris et al. 2013a).

REFERENCES

Abbot D. S., Cowan N. B., Ciesla F. J., 2012, ApJ, 756, 178
Alibert Y., 2014, A&A, 561, A41
Alibert Y., Carron F., Fortier A., Pfyffer S., Benz W., Mordasini C., Swoboda D., 2013, A&A, 558, A109
Ambrose D., 1956, Trans. Faraday Soc., 52, 772
Caldeira K., Wickett M. E., 2003, Nature, 425, 365
Charbonneau D. et al., 2009, Nature, 462, 891
Choukroun M., Grasset O., 2007, J. Chem. Phys., 127, 124506
Clough S. A., Kneizys F. X., Davies R. W., 1989, Atmos. Res., 23, 229
Cockell C. S., 1999, Planet. Space Sci., 47, 1487

Fortier A., Beck T., Benz W., Broeg C., Cessa V., Ehrenreich D., Thomas N., 2014, in Oschmann J. M., Jr Clampin M., Fazio G. G., MacEwen H. A., eds, Proc. SPIE Conf. Ser. Vol. 9143, Space Telescopes and Instrumentation 2014: Optical, Infrared, and Millimeter Wave. SPIE, Bellingham, p. 2

Fu R., O'Connell R. J., Sasselov D. D., 2010, ApJ, 708, 1326

Gardner J. P. et al., 2006, Space Sci. Rev., 123, 485

Gough D. O., 1981, Sol. Phys., 74, 21

Gueymard C. A., 2004, Sol. Energy, 76, 423

Kasting J. F., 1988, Icarus, 74, 472

Kasting J. F., Whitmire D. P., Reynolds R. T., 1993, Icarus, 101, 108

Kitzmann D., Patzer A. B. C., von Paris P., Godolt M., Stracke B., Gebauer S., Grenfell J. L., Rauer H., 2010, A&A, 511, A66

Komabayashi M., 1967, J. Meteor. Soc. Japan, 45, 137

Kopparapu R. K. et al., 2013, ApJ, 765, 131

Kuchner M. J., 2003, ApJ, 596, L105

Kunze M., Godolt M., Langematz U., Grenfell J. L., Hamann-Reinus A., Rauer H., 2014, Planet. Space Sci., 98, 77

Lammer H., Kasting J. F., Chassefière E., Johnson R. E., Kulikov Y. N., Tian F., 2008, Space Sci. Rev., 139, 399

Lammer H., Bredehöft J. H., Coustenis A., Khodachenko M. L., Kaltenegger L., Grasset O., 2009, A&AR, 17, 181

Léger A. et al., 2004, Icarus, 169, 499

Levi A., Sasselov D., Podolak M., 2014, ApJ, 792, 125

Li J., Scinocca J., Lazare M., McFarlane N., von Salzen K., Solheim L., 2006, J. Clim., 19, 6314

Manabe S., Strickler R. F., 1964, J. Atmos. Sci., 21, 361

Manabe S., Wetherald R. T., 1967, J. Atmos. Sci., 24, 241

Marboeuf U., Thiabaud A., Alibert Y., Cabral N., Benz W., 2014, A&A, 570, A36

Pierrehumbert R. T., 2010, Principles of Planetary Climate. Cambridge Univ. Press, Cambridge

Pierrehumbert R., Gaidos E., 2011, ApJ, 734, L13

Rauer H. et al., 2014, Exp. Astron., 38, 249

Ricker G. R. et al., 2014, in Oschmann J. M., Jr Clampin M., Fazio G. G., MacEwen H. A., eds, Proc. SPIE Conf. Ser. Vol. 9143, Space Telescopes and Instrumentation 2014: Optical, Infrared, and Millimeter Wave. SPIE, Bellingham, p. 20

Rothman L. S. et al., 2010, J. Quant. Spectrosc. Radiat. Transfer, 111, 2139

Rothschild L. J., Mancinelli R. L., 2001, Nature, 409, 1092

Simon F., Glatzel G., 1929, Z. Anorg. Allg. Chem., 178, 309

Stracke B., Godolt M., Grenfell J. L., Kitzmann D., von Paris P., Patzer A. B. C., Rauer H., 2015, Planet. Space Sci., submitted

Thiabaud A., Marboeuf U., Alibert Y., Cabral N., Leya I., Mezger K., 2014, A&A, 562, A27

Toon O. B., McKay C. P., Ackerman T. P., Santhanam K., 1989, J. Geophys. Res., 94, 16287

von Paris P. et al., 2010, A&A, 522, A23

von Paris P., Selsis F., Kitzmann D., Rauer H., 2013a, Astrobiology, 13, 899

von Paris P., Grenfell J. L., Rauer H., Stock J. W., 2013b, Planet. Space Sci., 82, 149

von Paris P., Grenfell J. L., Hedelt P., Rauer H., Selsis F., Stracke B., 2013c, A&A, 549, A94

Walker J. C. G., Hays P. B., Kasting J. F., 1981, J. Geophys. Res., 86, 9776

Wolf E. T., Toon O. B., 2013, Astrobiology, 13, 656

Wordsworth R. D., Pierrehumbert R. T., 2013, ApJ, 778, 154

This paper has been typeset from a TEX/LATEX file prepared by the author.